

Subtraction free arterial spin labeling: a new Bayesian-inference based approach for gaining perfusion data from time encoded data

Federico C A von Samson-Himmelstjerna^{1,2}, Michael A Chappell³, Jan Sobesky², and Matthias Günther¹

¹Fraunhofer MEVIS, Bremen, Bremen, Germany, ²Center for Stroke Research (CSB), Charité University Medicine Berlin, Berlin, Berlin, Germany, ³Institute of Biomedical Engineering & FMRIB Centre, University of Oxford, Oxfordshire, United Kingdom

Target audience: Researchers and clinicians interested in new acquisition techniques and developments of ASL

Purpose: Hadamard time-encoded pCASL (TE pCASL)¹ was recently introduced as an extension to arterial spin labeling (ASL) using encoding of the label to obtain perfusion kinetics in a time efficient manner. In general, from N encoding steps perfusion signals at $N-1$ different points in time can be decoded, with classical ASL corresponding to the special case $N=2$. Decoding consists of N different combinations of additions and/or subtractions of all N encoded images. In this scheme all N images are needed for correct decoding, missing or corrupted encoded images can render the entire dataset useless. An approach to increase the robustness was presented recently but with lower temporal resolution and SNR².

We propose a model for the encoded signal and use this in combination with Bayesian inference. This makes it possible to measure cerebral blood flow (CBF) and arterial transit time (ATT) even from incomplete or corrupted datasets. Furthermore, these data can be obtained without applying arithmetic operations like subtraction or addition reducing the sensitivity to subtraction/addition errors. We demonstrate the feasibility of the method and its capability to cope with incomplete datasets, which renders this approach especially suitable for the clinical setup where corrupted or missing data, e.g. by motion, is a frequent cause of lost diagnostic information.

Methods: Modeling: The model for the signal of the encoded data was based on the General Kinetic Model³ and describes the signal as a convolution of an arterial input function (AIF), describing the encoded blood bolus, and a tissue response function (TRF), e.g. as given in (3). Here, a box-car bolus shape was assumed and a Hadamard encoding scheme chosen, although other bolus shapes and encoding schemes can be employed. To account for the signal of static tissue + non-labeled (control) blood a constant term $S_{T,B}$ was added and the contribution of the labeled blood, reducing the signal intensity, was subtracted from this term:

$$S_j = S_{T,B} - \sum_k H_{jk} \cdot M_0 \cdot f \cdot (AIF(\tau) \otimes TRF)|_{Tl_k}$$

where Tl_k = subbolus length (SBL) + post labeling delay (PLD) of the k -th subbolus. The model was then implemented in FABBER/BASIL⁴ for Bayesian inference with FSL⁵. From the $N=8$ Hadamard-encoded images (fig. 1 a) CBF-, BAT- and $S_{T,B}$ -maps were generated (fig 1 b) I, II & III.

Imaging: For encoding an 8x7 Walsh-ordered Hadamard-matrix with an SBL of 350 ms and a PLD of 200 ms was used. The labeling plane was positioned at the height of the C3 vertebra, as perpendicular to the carotid and vertebral arteries as anatomy allowed. Standard two FOCI pulse background suppression was used and the measurement repeated 4 times for averaging. A 3D GRASE readout (res. = $2 \times 2 \times 5$ mm³ (native: $4 \times 4 \times 5$ mm³), matrix: 64x48, slices: 24, segments: 4, TA: 5:20 min) was employed. Image distortions originating from local B_0 -inhomogeneities were corrected using TOPUP^{6,7}. To do so, 2 M₀ images with the same readout as above but opposite phase encoding direction were acquired. After informed written consent volunteers were scanned at 3T (Skyra, SIEMENS Healthcare, Germany) using a 16-channel head coil.

Testing: To test the feasibility of the method reference CBF- and ATT-maps were created from a classical multi-TI fit in FABBER using the decoded TE pCASL images, i.e. perfusion maps for 7 different PLDs. Furthermore, to test the performance on incomplete datasets CBF-, ATT- and $S_{T,B}$ -maps from the new model were generated using a test dataset missing the last two images. Maps from the full and the incomplete datasets were then compared to the reference maps and to each other.

Results and Discussion:

Fig. 1a) shows the Hadamard encoded images as well as the model signal curve over the encoding steps (row of the matrix) in one voxel. Fig. 1c) shows the corresponding classical multi TI series obtained after decoding the encoded Hadamard images, as well as the signal curve over time of image acquisition in one voxel. From both datasets CBF- and ATT-maps were determined using Bayesian inference in FABBER for the classical multi TI (fig. 1d) I & II) as well as for the newly developed model where in addition a $S_{T,B}$ -map could be generated (fig. 1 b), I, II & III).

In summary, the CBF- and ATT-maps from the encoded-only images could successfully be created without applying any arithmetic operations like subtraction or addition. They agreed very well with the reference maps obtained classically from a multi TI dataset. Only small differences were found in ventricular regions which might originate from pulsatility of the cerebrospinal fluid (CSF) that is better attenuated by the averaging effect of decoding. Also for the incomplete test dataset good agreement with the reference method was found (images not shown). Compared to the full dataset only very small differences were observed, mainly in CSF regions. The $S_{T,B}$ maps were compared with the first encoded image, that is a pure control image and thus contains only signal from tissue + fully relaxed blood and here good agreement was found too.

Conclusion: Bayesian inference in combination with a Hadamard signal model makes it possible to obtain hemodynamic information like CBF and ATT, even from incomplete or corrupt datasets. This renders the approach especially suitable for the clinical setup where data corruption e.g. by motion is a common confounder. Furthermore, no subtractions or additions have to be performed and the postprocessing pipeline becomes shorter and thus easier and less error prone.

References: 1) Günther, ISMRM 2007, 380 2) von Samson-Himmelstjerna, ISMRM-ESMRMB 2014, 6229 3) Buxton, MRM 1998, 40(3),383:96 4) Chappell, IEEE Trans Signal Process 2009, 57(1),223:236 5) Jenkinson, Neuroimage 2012, 62(2),782:90 6) Andersson, Neuroimage 2003, 20(2),870:88 7) De Vito, ISMRM-ESMRMB 2014, 4558

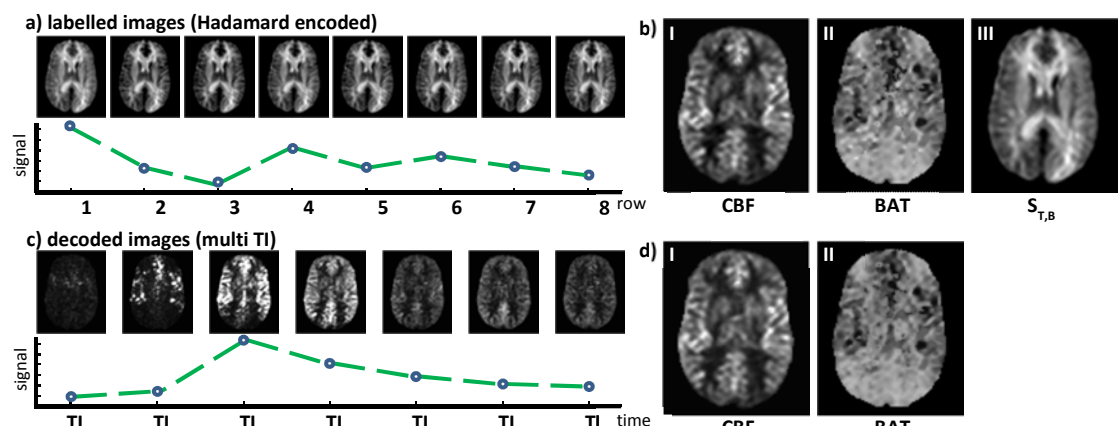


Figure 1: a): Hadamard encoded images and voxelwise signal curve over encoding steps (rows of Had.- matrix), b): I. CBF-, II. ATT- and III. $S_{T,B}$ -map generated from the images in a) using new model and BASI, c): decoded images for 7 different TIs and voxelwise signal curve over time, d): I. CBF- and II. ATT-map generated from the images in d) using classical multi-TI BASIL